Dalton Transactions

PAPER

View Article Online
View Journal | View Issue

Cite this: *Dalton Trans.*, 2014, **43**, 1524

A spectroscopic study on the coordination and solution structures of the interaction systems between biperoxidovanadate complexes and the pyrazolylpyridine-like ligands†

Xian-Yong Yu,*[a] Lin Deng,[a] Baishu Zheng,[a] Bi-Rong Zeng,[b] Pinggui Yi*[a] and Xin Xu*[c,d]

In order to understand the substitution effects of pyrazolylpyridine (pzpy) on the coordination reaction equilibria, the interactions between a series of pzpy-like ligands and biperoxidovanadate ($[OV(O_2)_2(D_2O)]^-$/$[OV(O_2)_2(HOD)]^-$, abbrv. bpV) have been explored using a combination of multinuclear (^1H, ^{13}C, and ^{51}V) magnetic resonance, heteronuclear single quantum coherence (HSQC), and variable temperature NMR in a 0.15 mol L^{-1} NaCl D_2O solution that mimics the physiological conditions. Both the direct NMR data and the equilibrium constants are reported for the first time. A series of new hepta-coordinated peroxidovanadate species $[OV(O_2)_2L]^-$ (L = pzpy-like chelating ligands) are formed due to several competitive coordination interactions. According to the equilibrium constants for products between bpV and the pzpy-like ligands, the relative affinity of the ligands is found to be pzpy > 2-Ester-pzpy ≈ 2-Me-pzpy ≈ 2-Amide-pzpy > 2-Et-pzpy. In the interaction system between bpV and pzpy, a pair of isomers (**Isomers A** and **B**) are observed in aqueous solution, which are attributed to different types of coordination modes between the metal center and the ligands, while the crystal structure of $NH_4[OV(O_2)_2(pzpy)]\cdot 6H_2O$ (**CCDC 898554**) has the same coordination structure as **Isomer A** (the main product for pzpy). For the N-substituted ligands, however, **Isomer A** or **B** type complexes can also be observed in solution but the molar ratios of the isomer are reversed (*i.e.*, **Isomer B** type is the main product). These results demonstrate that when the N atom in the pyrazole ring has a substitution group, hydrogen bonding (from the H atom in the pyrazole ring), the steric effect (from alkyl) and the solvation effect (from the ester or amide group) can jointly affect the coordination reaction equilibrium.

Received 22nd July 2013,
Accepted 21st October 2013

DOI: 10.1039/c3dt51986d

www.rsc.org/dalton

Introduction

In the last four decades, vanadium complexes, in particular, heteroligand peroxidovanadate complexes, have received increasing attention because they could act as an inorganic co-factor or a catalytic center involved in many enzymatic processes such as haloperoxidation, nitrogen fixation, *etc.*[1–4]

As peroxidovanadates and the corresponding complexes can inhibit protein tyrosine phosphatase (PTPase) and cause DNA cleavage both *in vitro* and *in vivo*, they have been tested as potential insulin-mimetic agents,[1–3,5] as well as anti-tumor drugs.[6] Being model compounds for haloperoxidases, peroxidovanadates could also oxidize organic or inorganic substrates to the corresponding products under mild conditions with high yield and remarkable selectivity. Therefore, the synthesis and characterization of peroxidovanadates and the investigation of their biological mechanisms have recently become the subject of extensive studies.[1–12] In these studies, the coordination chemistry of the peroxidovanadate complexes is

[a]*Key Laboratory of Theoretical Chemistry and Molecular Simulation of Ministry of Education, Hunan Province College Key Laboratory of QSAR/QSPR, School of Chemistry and Chemical Engineering, Hunan University of Science and Technology, Xiangtan 411201, China. E-mail: yu_xianyong@163.com, pgyi@hnust.cn; Fax: +86-731-58290509*

[b]*Department of Materials Science and Engineering, Key Laboratory for Fire Retardant Materials of Fujian Province, Xiamen University, Xiamen 361005, China*

[c]*Shanghai Key Laboratory of Molecular Catalysis and Innovative Materials, MOE Laboratory for Computational Physical Science, Department of Chemistry, Fudan University, Shanghai, 200433, China*

[d]*State Key Laboratory of Physical Chemistry of Solid Surfaces, College for Chemistry and Chemical Engineering, Xiamen University, Xiamen 361005, China. E-mail: xxchem@fudan.edu.cn*

†Electronic supplementary information (ESI) available: The experimental procedures and spectroscopic data of ligands **1**–**5** and complex **6**. CCDC 898554. For ESI and crystallographic data in CIF or other electronic format see DOI: 10.1039/c3dt51986d

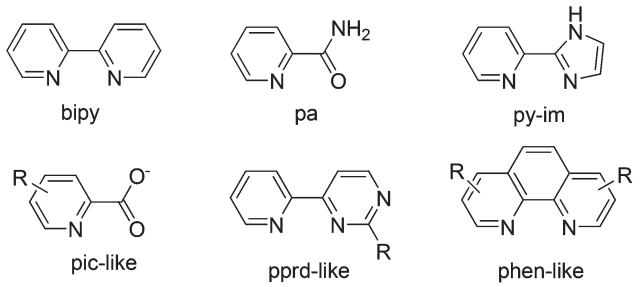

Scheme 1 The structures of some classic heteroligands in the peroxidovanadate complexes.[5,10,11c,d,12f]

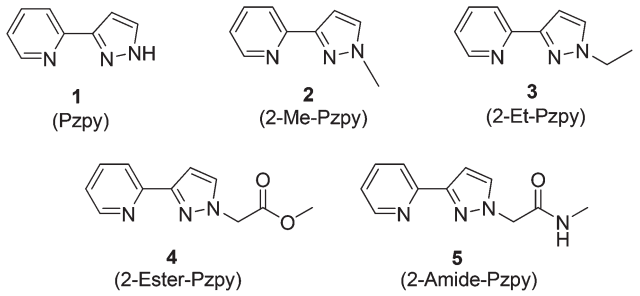

Scheme 2 The structures of the pyrazolylpyridine (pzpy)-like ligands **1–5**.

the main concern.[3,9–12] For example, Matsugo and co-workers have synthesized several novel peroxidovanadate(v) compounds containing amino acid derivatives and have studied their physiological effects.[7a] A novel vanadium(v) oxoperoxido complex containing the 2-acetylpyridine thiophene-2-carboxylic hydrazone ligand has been synthesized and characterized by Zhou's group.[7b] And their study indicated that the crystal structure is stabilized by intermolecular hydrogen bonding.[7b] A unique dinuclear mixed V(v) oxo–peroxo complex in the structural speciation of the ternary V(v)–peroxo–citrate system has been explored by Salifoglou's group.[7c] At the same time, they have also studied the possible mechanism and structure to explore the aqueous synthetic chemistry of a dinuclear V(v)–citrate–H_2O_2 system. Mayer and co-workers have synthesized and studied the reactivity of the oxo–peroxo–vanadium(v) bipyridine compounds.[7d] A series of peroxidovanadate complexes containing heteroligands such as nitrilotriacetic acid, 2,2′-bipyridine, 1,10-phenanthroline, and picolinate have been synthesized and characterized as functional models for the vanadium haloperoxidase enzymes[9] or as potential insulin-mimetic agents.[5,10] Furthermore, peroxidovanadates containing 2-(2-pyridyl)-imidazole or picolinamide ligands have been successfully synthesized and characterized by Chen's group.[11c,d] The structures of some classic heteroligands in peroxidovanadate complexes are shown in Scheme 1.[5,10,11c,d,12f] As revealed by the studies from Pettersson's or Rehder's groups,[12a–g] it is particularly important to choose these chelating ligands which contain the pyridine (py) building block in synthesizing the peroxidovanadate complexes.

The pyrazolylpyridine (abbr. pzpy) ligand, which has both the py ring and the pyrazole (pz) ring, is analogous to 2-(2-pyridyl)-imidazole in terms of the chelating site and is expected to be a good ligand for peroxidovanadate complexes. There are reports in the literature showing that pzpy could coordinate with a series of metal ions such as Mn^{2+},[13a] Fe^{2+},[13b] Co^{2+},[13c] Ni^{2+},[13c,d] Cu^{2+},[13e] Zn^{2+},[13c,f] Mo^{6+},[13g] Rh^{+},[13h] Ru^{2+},[13i] Cd^{2+},[13f,i] Pt^{2+},[13j] and Au^{3+}.[13k] In the present work, a series of the pzpy-like ligands (**1–5**, shown in Scheme 2) have been synthesized, which have been used to investigate the substitution effects of the pzpy ligand on the coordination reaction equilibrium with peroxidovanadate. We have explored the interactions between $[OV(O_2)_2(D_2O)]^-$/$[OV(O_2)_2(HOD)]^-$ (abbr. bpV) and the pzpy-like ligands in a 0.15 mol L^{-1} NaCl D_2O solution that mimics the physiological conditions by means of multinuclear (^1H, ^{13}C, and ^{51}V) magnetic resonance, heteronuclear single quantum coherence (HSQC), and variable temperature NMR. For the pzpy (**1**) ligand, a new single crystal (NH_4-$[OV(O_2)_2(pzpy)]\cdot 6H_2O$, **CCDC 898554**) was obtained and has been characterized using spectroscopic methods. By combining the above mentioned methods and comparing the crystal structures of all the different species, their solution structures and coordination modes in the interacting systems have been determined; thereafter a better understanding has been achieved which suggests that the coordination equilibria in solution are influenced by hydrogen bonding (from the H atom in the pz ring), the steric effect (from alkyl) and the solvation effect (from the ester or amide group).

Results and discussion

Solid state structure of 6

Crystal **6** consists of ammonium ions, pzpy ligand-coordinated biperoxidovanadate(v) complexes and water of crystallization, held together by ionic and hydrogen bond interactions.

The structure of $[OV(O_2)_2(pzpy)]^-$ is depicted in Fig. 1, which shares a distorted pentagonal bipyramidal geometry. The four peroxido oxygens (O1, O2, O3 and O4), as well as the nitrogen atom (N2) in the pz ring, define an equatorial plane with respect to the axial V=O bond within the limits of experimental error. The nitrogen atom (N1) in the pyridine ring binds to V in the axial position. Listed in Table 1 are some selected bond lengths of complex **6**, and the corresponding values of other biperoxidovanadate complexes are also shown in the table for comparison. More detailed structural data of complex **6** can be found in ESI as presented in Table S1.†

The axial V=O length is 1.597 Å for **6** as shown in Table 1. This value is typically found for a double bond between V and O atoms and is within the range observed in similar geometries such as those of $[OV(O_2)_2(pic)]^-$ and $[OV(O_2)_2(2\text{-}NH_2\text{-}pprd)]^-$.[10,12f] The 0.33 Å displacements of the vanadium atom from the equatorial plane are comparable to that of ~0.3 Å, found in other hepta-coordinated biperoxidovanadate complexes.[11c,14] The $V\text{–}O_{peroxido}$ bond lengths are around 1.865–1.922 Å which are also within the range of the normal $V\text{–}O_{peroxido}$ bond distances as reported in $[OV(O_2)_2(py\text{-}im)]^-$

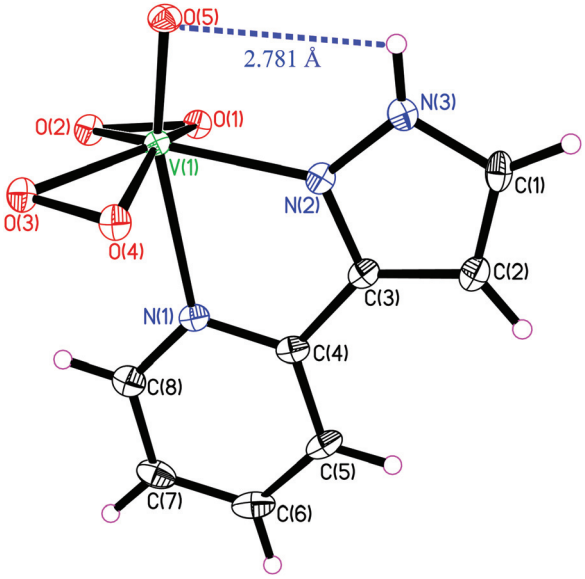

Fig. 1 Structures of the pzpy-like ligand-coordinated peroxidovanadate complexes in the $NH_4[OV(O_2)_2(pzpy)]\cdot 6H_2O$ (**6**) crystals. Ammonium ions and waters of crystallization are not shown.

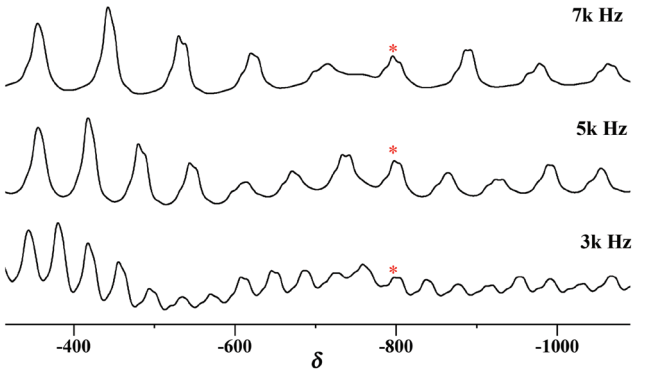

Fig. 2 Solid-state ^{51}V NMR spectra of **6**. The asterisk indicates the ^{51}V NMR signal; other bands are spinning side-bands.

and $[OV(O_2)_2(pprd)]^-$.[11c,12f] The lengths of the $(O–O)_{peroxido}$ bonds are within the range of 1.451–1.456 Å, similar to the corresponding values in $[OV(O_2)_2(pic)]^-$ and $[OV(O_2)_2(bipy)]^-$.[10,14e] The bond lengths for both $V–N_{equatorial}$ (2.086 Å) and $V–N_{axial}$ (2.370 Å) are in good agreement with the corresponding values found for other peroxidovanadate complexes such as $[OV(O_2)_2(pic)]^-$, $[OV(O_2)_2(py\text{-}im)]^-$, and $[OV(O_2)_2(bipy)]^-$.[10,11c,14e]

The ^{51}V MAS NMR spectra of **6** are shown in Fig. 2 at the spinning rates of 3, 5, and 7 kHz, respectively. Its chemical shift is located at −796 which is different from that of **Isomer A** in solution (chemical shift located at −774 at 20 °C, see below). The shielding differences may be imparted by the nature of the ligands/the ligand sphere in crystals or in solutions.

Solution state structures of 6

X-ray diffraction provides conclusive results for the coordination modes of **6** in the solid state. However, its solution state structures need to be further explored by using solution NMR spectra. The details of ^1H and ^{13}C NMR spectroscopic data for **6** in solutions can be found in ESI.†

Fig. 3 shows the variable temperature ^1H NMR spectra of complex **6**. From Fig. 3 it is clear that: (1) the spectra are quite broad at room temperature, and become much more sharp at the temperature range of 1–6 °C, (2) the low temperature signals can be grouped mainly into two sets, one stronger and the other weaker, and (3) the signals of the trace free pzpy are very weak and will be explored in the following section.

A comparison between ^{13}C NMR spectra of **6** in solution (a) and that in the solid state (b) is shown in Fig. 4. As seen in Fig. 4, this comparison seems to be not so straightforward. Obviously, the signals in solution can also be grouped into two sets, one stronger (labeled with *) and the other weaker. We will assume that when complex **6** is dissolved in solution, there exists a pair of isomers (**A** and **B**). The set of stronger signal peaks are to be attributed to **Isomer A**, which is the main product in solution and may adopt the same coordination mode as that in the solid state of **6**. **Isomer B**, which gives rise to the set of weaker signal peaks, would adopt a different coordination mode as compared to that in the solid state and it is the minor product in solution. By a careful examination of the crystal structure in Fig. 1, we propose that **Isomer B** may have an interchanged coordination mode with $N_{equatorial}$ and N_{axial}, *i.e.*, it is the nitrogen atom (N2) in the pz ring, instead of that (N1) in the py as in **Isomer A**, that

Table 1 Selected bond lengths of **6** as well as those of the other peroxidovanadate complexes

	bpV(pzpy)	bpV(pprd)	bpV(2-NH_2-pprd)	bpV(pic)	bpV(py-im)	bpV(bipy)
V=O	1.597(3)	1.611(3)	1.606(3)	1.599(4)	1.614(2)	1.619(3)
$V–O_{peroxo(trans)}$	1.877(3)	1.895(2)	1.882(4)	1.895(4)	1.891(2)	1.883(3)
	1.865(3)		1.878(4)	1.881(4)	1.879(2)	1.880(3)
$V–O_{peroxo(cis)}$	1.922(3)	1.887(2)	1.912(4)	1.917(4)	1.918(2)	1.911(3)
	1.920(3)		1.901(3)	1.899(4)	1.899(2)	1.909(3)
$(O–O)_{peroxo}$	1.456(4)	1.472(3)	1.473(6)	1.464(5)	1.462(3)	1.471(4)
	1.451(4)		1.465(5)	1.458(6)	1.449(3)	1.465(4)
$V–N_{equatorial}$	2.086(4)	2.142(3)	2.128(4)	2.123(5)	2.102(3)	2.149(4)
$V–N/O_{axial}$	2.370(4)	2.332(3)	2.400(4)	2.290(4)	2.356(3)	2.288(3)
Ref.	This work	12*f*	12*f*	10	11*c*	14*e*

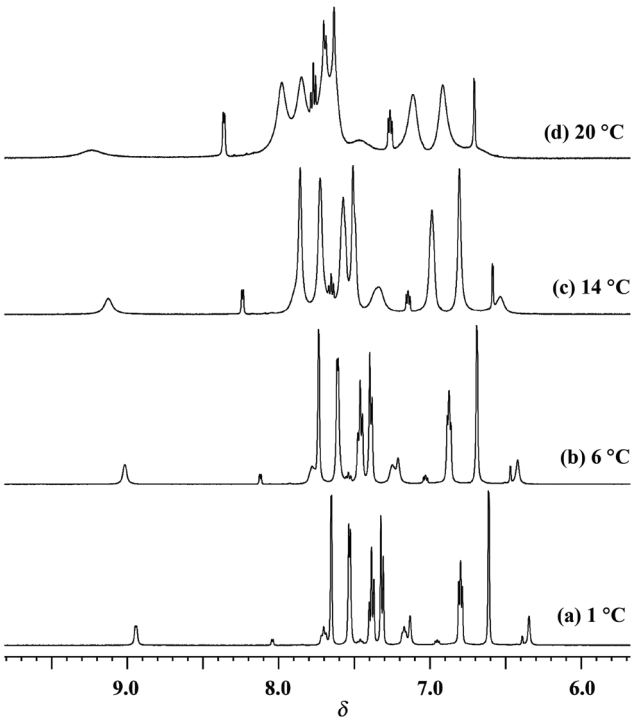

Fig. 3 Variable temperature ^{1}H NMR spectra of complex **6** in aqueous solution.

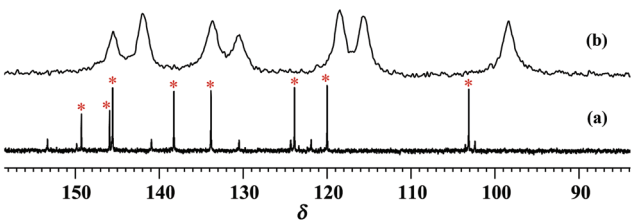

Fig. 4 ^{13}C NMR spectra: complexes **6** in solution (at 1 °C, a) and in solid-state (at room temperature, b).

binds to V in the axial position in **Isomer B**. Similar phenomena have been observed when bpV binds to the 4-(pyridin-2-yl)-pyrimidine-like ligands.[12f]

To better understand the reasons for the coordination differences in crystals and in solutions, we will ascertain the coordination modes associated with **Isomers A** and **B** to explore their formation mechanisms. In the following sections, we will also discuss the substitution effects on the coordination reaction equilibria of a series of pzpy-like ligands (**1–5**) to biperoxidovanadates.

^{1}H and ^{13}C NMR data of the interaction systems between bpV and the pzpy-like ligands

In order to investigate the coordination ways between the metal center vanadium and pzpy (**1**) in detail, the bpV–pzpy-like ligand interaction systems were studied by using variable temperature ^{1}H and ^{13}C NMR spectra. For the pzpy (**1**) ligand, we used the solution of complex **6** as the bpV–pzpy interaction system (the molar ratio is 1 : 1). For other pzpy-like ligands, the

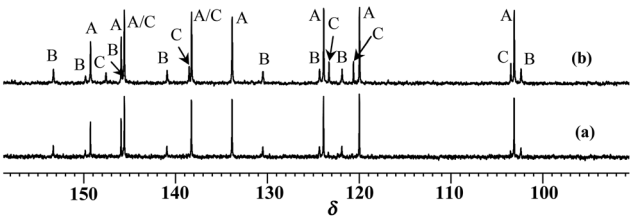

Fig. 5 ^{13}C spectra of the bpV–pzpy interaction systems in aqueous solution at 1 °C. The molar ratio of bpV and pzpy is 1 : 1 and 1 : 1.2 in (a) and (b), respectively. A, B and C label the signals from **Isomer A**, **Isomer B** and the free pzpy (**1**) ligand, respectively.

bpV solution was first prepared according to the procedure described in the Experimental section and then varied amounts of the pzpy-like ligands (**2–5**) were added.

Shown in Fig. 5 are the ^{13}C spectra of the bpV–pzpy interaction systems in aqueous solution at 1 °C. The molar ratio of bpV and pzpy is 1 : 1 and 1 : 1.2 in (a) and (b), respectively. In Fig. 5(a), there exist mainly two sets of peaks. These are identical to those in Fig. 3(a) for the solution of **6**. However, when the amount of pzpy (**1**) was increased (from 1 to 1.2 equivalents), peaks of free pzpy ligands appeared. These are clearly seen in Fig. 5(b). Therefore, we assign the set of stronger signals as an indication of the formation of **Isomer A**, and the set of weaker signals as an indication of the formation of **Isomer B**. Based on the assignment of ^{13}C NMR signals, the ^{1}H NMR signals of the bpV–pzpy interaction systems can also be assigned using the HSQC spectrum as displayed in Fig. 6.

NMR (^{1}H, ^{13}C and ^{51}V) results for the other interaction systems between bpV and the pzpy-like ligands (**2–5**) are summarized in Table S2 in ESI.† The changes of the ^{1}H and ^{13}C

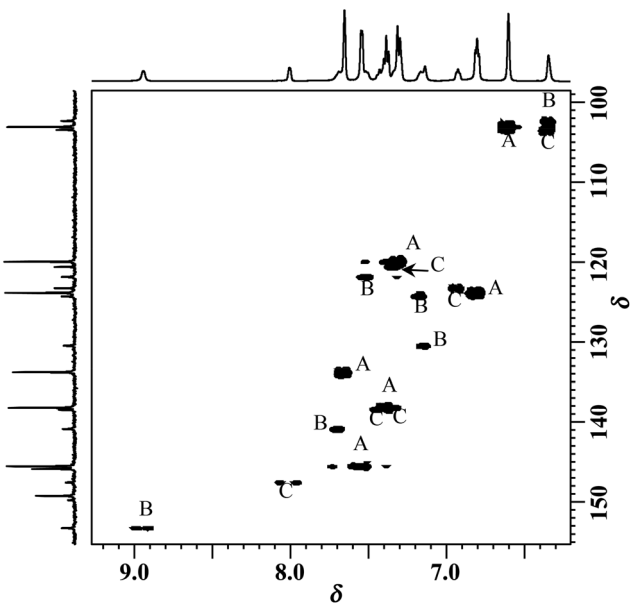

Fig. 6 HSQC spectrum of the bpV–pzpy interaction systems in aqueous solution. The molar ratio of bpV and pzpy is 1 : 1.2. A, B and C label the signals from **Isomer A**, **Isomer B** and the free pzpy (**1**) ligand, respectively.

chemical shifts of organic ligands before/after coordination reaction suggest that ligands (**2–5**) indeed coordinate to bpV and have similar coordination models to that of pzpy in solution. According to the spectroscopic results from NMR or X-ray diffraction, these *N*,*N*′-chelating biheteroaromatic ligands shall form the hepta-coordinated $[OV(O_2)_2L]^-$ (L = pzpy-like ligands) species as exemplified by $[OV(O_2)_2(py\text{-}im)]^-$, $[OV(O_2)_2(pprd)]^-$, or $[OV(O_2)_2(2\text{-}NH_2\text{-}pprd)]^-$ studied previously.[11c,12f]

^{51}V NMR of the interaction systems between bpV and the pzpy-like ligands

Table S2† summarizes the ^{51}V NMR results for the interaction systems between bpV and the pzpy-like ligands (**1–5**), which we will discuss in detail in this section. It was reported that the as-prepared bpV (see the Experimental section) has a ^{51}V peak located at −692 ppm at 20 °C (see Fig. 7(a)).[15] When the pzpy ligand was added to the bpV solution, new peaks appeared at about −738 and −774 ppm (see Fig. 7(b)–(d)), which indicates the formation of bpV–pzpy complexes $[OV(O_2)_2(pzpy)]^-$. In the bpV–pzpy interaction systems, **Isomer A**, corresponding to the upfield peak, is the major product, while **Isomer B**, corresponding to the low field peak, is the minor product. The intensities of these newly-formed peaks increase with the increase of the molar ratio of pzpy over bpV (from 0 to 0.5, 1, and finally to 1.2 equivalents) before it reaches a maximum, as presented in Fig. 7(b)–(d). It is worth mentioning that the molar ratio of **Isomer A** to **B** is still kept at 3.2 : 1 in the process of adding more pzpy (**1**) into the solution at a temperature of 20 °C. These results are consistent with those of ^{1}H and ^{13}C NMR spectra of **6** dissolved in solution as well as those of the bpV + pzpy (**1**) systems. The conclusion that there are two types of coordination modes existing when the pzpy ligand (**1**) binds to the metal center as indicated by the appearance of two sets of peaks for the species of $[OV(O_2)_2(pzpy)]^-$ in the NMR spectra is, therefore, further supported.

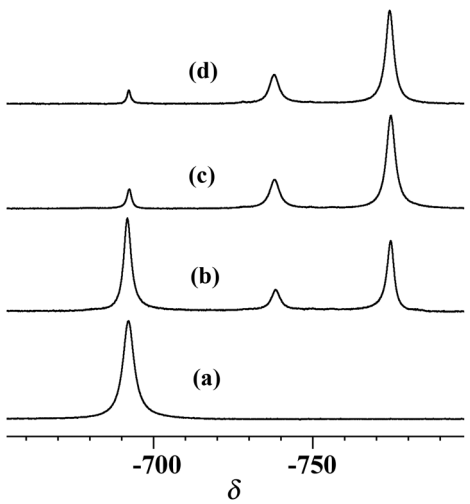

Fig. 7 The ^{51}V NMR spectra of the interaction systems between bpV and pzpy (**1**) in aqueous solution at 20 °C. (a)–(d) correspond to the molar ratios of pzpy/bpV = 0, 0.5, 1.0, and 1.2, respectively.

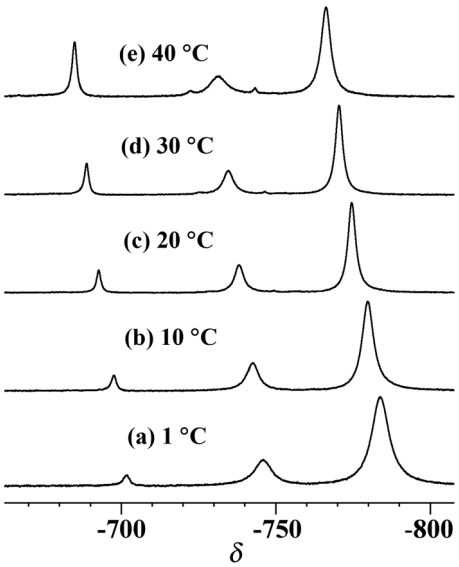

Fig. 8 Variable temperature ^{51}V NMR spectra of the complex **6** solution.

In order to investigate how temperature influences the coordination equilibrium, the variable temperature ^{51}V NMR spectra of the solution of complex **6**, which can be considered as the interaction system between bpV and pzpy (**1**) with a 1 : 1 molar ratio, was studied in the temperature range of 1–40 °C. The results are displayed in Fig. 8, which show that: (1) with the increase of temperature, all peaks move towards low field. The chemical shift of bpV moves about 4.5 ppm every 10 °C and that of **Isomer A** or **B** moves about 4.5 or 3.6 ppm, respectively, every 10 °C; (2) with the increase of temperature, the quantity of $[OV(O_2)_2(pzpy)]^-$ species decreases, due to its conversion into bpV. At the same time, the ratio between **Isomers A** and **B** decreases (4 : 1 at 1 °C and 2.8 : 1 at 40 °C). This suggests that with an increase of temperature, $[OV(O_2)_2(pzpy)]^-$ is converted back into bpV gradually, and **Isomer A** is also converted into **Isomer B**. Coincidently, the variable temperature ^{1}H NMR spectra shown in Fig. 3 also suggest that the peaks of free pzpy increase with the increase of temperature, which agrees with the experimental results of the variable temperature ^{51}V NMR spectra.

Fig. 9 displays the respective ^{51}V NMR spectra for all pzpy-like ligands (**1–5**) at 1 °C, which reveals how the N-substitution groups in the pz ring affect the coordination equilibrium with bpV. Fig. 9 shows that when the corresponding pzpy-like ligands are added, the intensity of the bpV peak decreases and new peaks appear. For pzpy (**1**) shown in Fig. 9(a), peaks at −745 and −783 ppm are assigned to $[OV(O_2)_2(pzpy)]^-$. For 2-Me-pzpy (**2**) shown in Fig. 9(b), new peaks at about −743 and −775 ppm are assigned to $[OV(O_2)_2(2\text{-Me-pzpy})]^-$. Similarly, there are newly-formed peaks presented in Fig. 9(c)–9(e) at −741 and −773 ppm, −737 and −761 ppm, −740 and −760 ppm, respectively, which are assigned to $[OV(O_2)_2(2\text{-Et-pzpy})]^-$, $[OV(O_2)_2(2\text{-Ester-pzpy})]^-$, and $[OV(O_2)_2(2\text{-Amide-pzpy})]^-$, accordingly. At the same time, there are small new

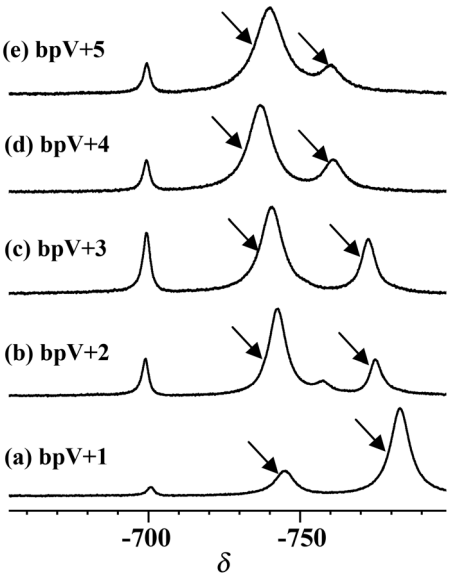

Fig. 9 ^{51}V NMR spectra of the interaction systems of bpV and the pzpy-like ligands (**1–5**) in aqueous solution at 1 °C. Peaks of the newly formed $[OV(O_2)_2L]^-$ (L = **1–5**) species are indicated by arrows.

peaks at −756 ppm shown in Fig. 9(b), which might be assigned to the ligand-free peroxidovanadate $[HV_2O_3(O_2)_4]^{3-}$ according to a literature report.[16] These assignments of the pzpy-like ligand coordinated ^{51}V peaks can be confirmed by analyzing their fluorescence quenching with the increase in bpV concentration (see below for further discussion). Based on the ratios of bpV peak areas before and after coordination reactions, the relative affinity of the pzpy-like ligands towards bpV was determined to be **1** > **4** ≈ **2** ≈ **5** > **3**.

Quantitative measurements of the formation constants for the interaction systems between bpV and the pzpy-like ligands

To achieve a quantitative evaluation of the coordination affinity of the ligands, the formation constant of bpV and a pzpy-like ligand is determined by analyzing the fluorescence quenching of the pzpy-like ligand with the increase of the bpV

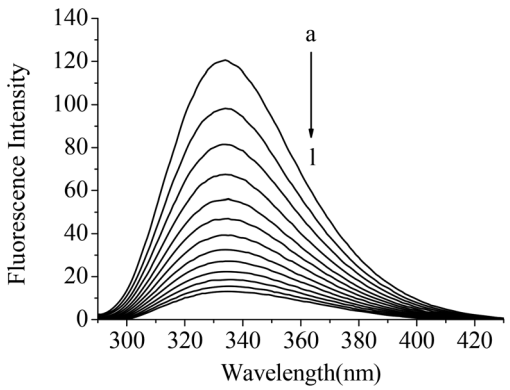

Fig. 10 The fluorescence emission spectra of pypz (1×10^{-4} mol L^{-1}) with different concentrations of bpV. (*a* ~ l): [bpV] = 0, 1, 2–12 × 10^{-4} mol L^{-1} (λ_{ex} = 286 nm).

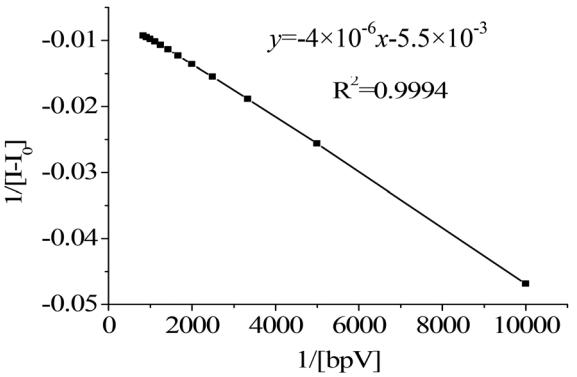

Fig. 11 Fluorescence spectra of the Benesi–Hildebrand plot for the interaction between pypz and bpV.

Table 2 The equilibrium constants for coordination between bpV and the pzpy-like ligands. Note that the linear correlation coefficient R^2 is generally higher than 0.999 at 30 °C

Systems	*K*	R^2
bpV + pzpy (**1**)	1375	0.9994
bpV + 2-Me-pzpy (**2**)	1200	0.9992
bpV + 2-Et-pzpy (**3**)	1100	0.9999
bpV + 2-Ester-pzpy (**4**)	1237	0.9994
bpV + 2-Amide-pzpy (**5**)	1175	0.9997

concentration. The results, when the ligand is pzpy, are presented in Fig. 10.

Since the molar ratio between bpV and the pzpy-like ligands in the newly-formed peroxidovanate complexes is 1 : 1, the formation constant can be analysed by using the Benesi–Hildebrand[17] equation:

$$\frac{1}{I - I_0} = \frac{1}{\alpha(I' - I_0)} + \frac{1}{K\alpha(I' - I_0)[\text{bpV}]} \quad (1)$$

where *K* is the formation constant, I_0 is the initial fluorescence intensity of the free pzpy-like ligands, I' is the minimum fluorescence intensity, and *I* is the observed fluorescence intensity. A plot of $1/(I - I_0)$ *vs.* 1/[bpV] is shown in Fig. 11 for the pzpy ligand. The formation constant can be obtained from the intercept and the slope according to eqn (1). The results are displayed in Table 2 for all ligands (**1–5**). The linear correlations are all excellent for the coordination reactions with all pzpy-like ligands. The data in Table 2 quantitatively evaluate the relative affinities between bpV and various pzpy-like ligands, which reconfirm the conclusion from the ^{51}V NMR spectra shown in Fig. 9 that the pzpy-like ligands (**1–5**) bind to bpV with the trend in binding affinity as **1** > **4** ≈ **2** ≈ **5** > **3**.

Coordination mechanisms between bpV and the pzpy-like ligands

In order to explore the coordination mechanisms, we first investigate the interactions between bpV and a series of organic molecules, which are the building blocks of the pzpy-like ligands, such as py, pz, and 1-methylpyrazole (1-Me-pz).

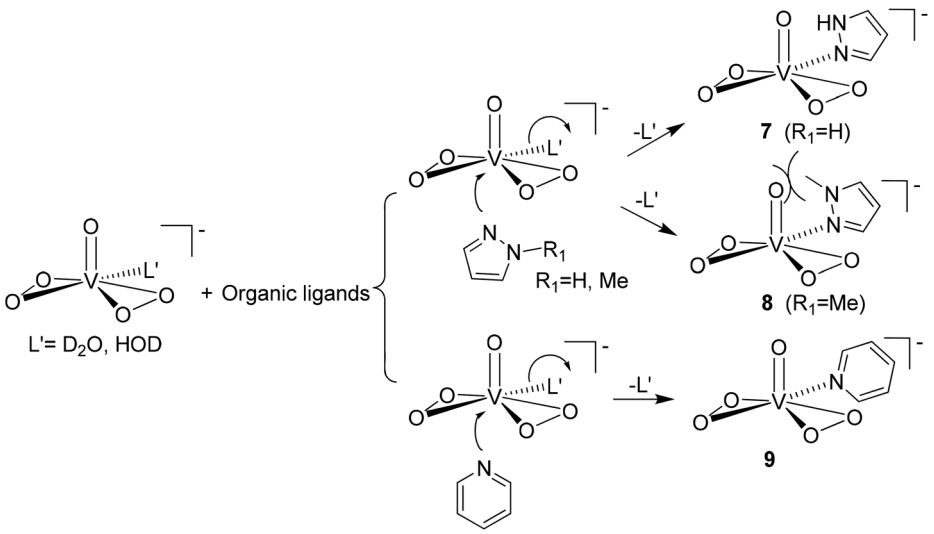

Scheme 3 The coordination modes between bpV and organic ligands such as pyridine, pyrazole or 1-methylpyrazole. ')(' in **8** indicates the steric interaction.

According to literature reports,[12f,15a] the relative binding affinity of the ligands towards bpV follows the trend as py ≈ pz > 1-Me-pz. The coordination modes between bpV and py, pz, or 1-Me-pz are summarized in Scheme 3. The above experimental results demonstrate that: (1) for these organic ligands, coordination to bpV leads to a series of hexa-coordinated peroxidovanadate species as shown in **7**–**9**, (2) for a pz ligand, coordination to bpV is always permissive, although the N-substitution group as shown in **8** will lead to a steric effect which will decrease the binding affinity, and (3) for a py ligand, however, coordination of an *ortho*-substituted ligand to bpV is permissive only when the substitution group is also a coordination group, such that the chelate effect enhances the stability of the complex.[12f]

According to our previous study[12f] and the Conte group's work,[18] a neutral monodentate ligand such as py or pz can coordinate to $[OV(O_2)_2]^-$ in two possible ways: one is that the ligand lies in the equatorial plane of the peroxide oxygens and the other is that the ligand is on the axis *trans* to the oxo group. Previous *ab initio* calculations suggested that the former is more favorable in energy than the latter.[18] For the pzpy-like bidentate ligands, we assume that the interaction process can be artificially decomposed into two steps (see Scheme 4). Because the coordination ability of the ligands is py ≈ pz > 1-Me-pz, both the py and the pz building blocks are expected to occupy the favorable equatorial position to form a hexa-coordinated complex, giving **Intermediate A** or **B**. Therefore, in the interaction systems between bpV and the pzpy-like ligands, both isomers of **A** and **B** type shall be observed. Therefore, for the pzpy ligand, the molar ratio between **Isomers A** and **B** shall be similar, as py and pz possess similar binding affinity to bpV. However, the observed ratio between **Isomers A** and **B** is actually 2.8 : 1 when the temperature is increased to 40 °C (in Fig. 8). In the crystal structure shown in Fig. 1, hydrogen bond interactions are evident, as shown by the distances of H3 in the N3 atom to O5 (2.781 Å). The hydrogen bond interactions help to improve the complex stability which gives rise to **Isomer A** as the major product. On the other hand, when the N-substituted pzpy-like ligands coordinate to bpV, the py ligand is expected to favorably occupy the equatorial position and to form a hexa-coordinated **Intermediate B**. This is due to the fact that the coordination ability of py is stronger than that of 1-Me-pz, because of the steric effect in the latter. **Isomer B** is eventually formed by binding the N-substituted pz building block to the metal center epaxially to form the hepta-coordinated structure (*i.e.*, **Route B** in Scheme 4). This explains why, for ligands **2**–**5**, complexes of **Isomer B** type are the main products.

It is known that pz binds strongly to bpV, while an *ortho* N-substituted group will reduce its binding affinity due to the steric effect. Hence, for 2-Me-pzpy and 2-Et-pzpy, the relative binding affinity follows the trend 2-Me-pzpy > 2-Et-pzpy. When the N-substituted ligand contains the ester/amide group, the additional effect plays a role in stabilizing the product. For 2-Ester-pzpy and 2-Amide-pzpy, both the steric effect and the solvation effect have affected the coordination reactions. To some extent, the favorable solvation effect can offset the otherwise steric repulsion; the relative affinity of 2-Ester-pzpy or 2-Amide-pzpy is close to that of 2-Me-pzpy, while better than that of 2-Et-pzpy. These conclusions agree with the results shown in Fig. 9 and Table 2 which shed light on the coordination mechanisms between bpV and the pzpy-like ligands in solutions. Hence, the ligand binding affinities follow the trend pzpy > 2-Ester-pzpy ≈ 2-Me-pzpy ≈ 2-Amide-pzpy > 2-Et-pzpy.

Conclusions

In this work, the interactions between biperoxidovanadate complexes (bpV) and a series of pyrazolylpyridine (abbr. pzpy)-

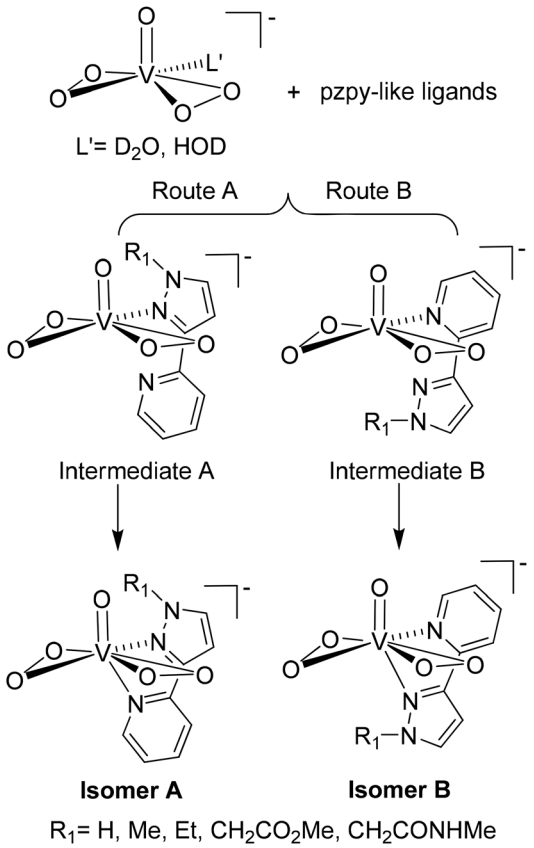

Scheme 4 Possible interaction modes between bpV and the pzpy-like ligands in solution.

like ligands in a 0.15 mol L^{-1} NaCl D_2O solution have been investigated by using several NMR experimental techniques. The relative affinity of the pzpy-like ligands was found to follow the trend pzpy > 2-Ester-pzpy ≈ 2-Me-pzpy ≈ 2-Amide-pzpy > 2-Et-pzpy. When the ligand was pzpy, a pair of isomers (**Isomers A** and **B**) were observed in aqueous solution, which have been attributed to different types of coordination modes between the metal and the ligands. **Isomer A** (the main product) has the same coordination structure as in the $NH_4[OV(O_2)_2(pzpy)]\cdot 6H_2O$ (**CCDC 898554**) crystal. For the N-substituted ligands, both complexes of **Isomers A** and **B** types have also been observed in solution. However, the molar ratio of the two isomers is reversed with **Isomer B** type being the main product. These results demonstrate that, for the N-substituted groups in the pyrazole ring, the hydrogen bonding (from the H atom in the pyrazole ring), the steric effect (from alkyl) and the solvation effect (from the ester or amide group) can join to significantly affect the coordination reaction equilibrium.

Experimental section

Materials and preparation

The compounds NH_4VO_3, H_2O_2, 4-(2-hydroxyethyl)-1-piperazine-ethane-sulfonic acid (HEPES), and NaCl were commercial products from Sinopharm Chemical Reagent Company without further purification. The pzpy-like ligands were synthesized according to a method reported in the literature.[19] The experimental procedures and spectroscopic data of these compounds have been summarized in ESI.†

To form the interaction systems between bpV and pzpy-like ligands, NH_4VO_3 and H_2O_2 were mixed with a 1 : 5 molar ratio to the bpV solution first. The respective ligands were then added to the solution. Unless otherwise stated, the total concentration of vanadate species is 0.2 mol L^{-1}.

The biperoxidovanadate crystals were prepared by adding 10 mL H_2O_2 (30%, w/v, solution) and 1.17 g NH_4VO_3 to 50 mL distilled water. After NH_4VO_3 was dissolved, 1.47 g pzpy was added to the mixture. The mixture was stirred in an ice water bath at 273 K for 0.5 h. The reaction mixture was then filtered and the solution was kept at 278–283 K for a week to crystallize. The yellow block crystals were filtered and washed with 2 mL cold water and 7 mL cold ethanol and then dried on a filter paper. The isolated yield was 50–70% based on the vanadate.

Crystal structure determination

Determination of the unit cell and data collection for biperoxidovanadate compound **6** (yellow block crystal, 0.45 × 0.16 × 0.10 mm) were performed on a Bruker SMART APEX CCD single-crystal diffractometer using graphite-monochromatized Mo Kα radiation (λ = 0.71073 Å) at 173 K. Crystal data and details of the data collection and refinement are shown in Table 3. The structures were solved using direct methods as implemented in the program SHELXS97. The non-hydrogen atoms were refined using the full-matrix least-square procedure on F^2. Anisotropic displacement parameters were assigned to non-hydrogen atoms.

CCDC 898554 contains the crystallographic data for **6**.

Table 3 Experimental crystal data and structure refinement parameters for $NH_4[OV(O_2)_2(pzpy)]\cdot 6H_2O$ (**6**)

Compound reference	**6**
Chemical formula	$C_8H_{23}N_4O_{11}V$
Formula mass	402.24
Crystal system	Monoclinic
a/Å	7.5216(17)
b/Å	26.293(6)
c/Å	9.411(2)
α/°	90.00
β/°	111.488(4)
γ/°	90.00
Unit cell volume/Å^3	1731.9(7)
Temperature/K	173(2)
Space group	$P21/a$
No. of formula units per unit cell, Z	4
No. of reflections measured	8593
No. of independent reflections	3029
R_{int}	0.0284
Final R_1 values ($I > 2\sigma(I)$)	0.0727
Final w$R(F^2)$ values ($I > 2\sigma(I)$)	0.1357
Final R_1 values (all data)	0.0735
Final w$R(F^2)$ values (all data)	0.1362
CCDC number	**898554**

Spectroscopic measurements

Room temperature solid-state NMR experiments were performed on a 300 MHz Bruker DMX NMR spectrometer, operating at 78.8 MHz for ^{51}V NMR and 75.5 MHz for ^{13}C NMR. The ^{51}V chemical shifts were referenced to $VOCl_3$, while the ^{13}C chemical shifts were referenced to the carbonyl carbon of glycine, which, in turn, is 173.2 ppm with respect to that of tetramethylsilane. IR spectra were recorded on a Perkin-Elmer spectrometer (Spectrum One).

The solution NMR spectra were recorded on a 500 MHz Bruker AV II NMR spectrometer operating at 500.13 MHz for ^{1}H NMR, 125.77 MHz for ^{13}C NMR and 131.47 MHz for ^{51}V NMR. DSS (3-(trimethylsilyl)-propanesulfonic acid sodium salt) was used as an internal reference for ^{1}H and ^{13}C chemical shifts. ^{51}V chemical shifts were measured relative to the external standard $VOCl_3$ with the upfield shifts considered as negative values. The signal-to-noise ratios were improved by a line-broadening factor of 2 Hz and 10 Hz in the Fourier transformation of all ^{13}C and ^{51}V spectra. In the NMR experiments, an ionic medium, 0.15 mol L^{-1} NaCl D_2O, was chosen in order to represent physiological conditions.

The equilibrium constants for coordination between bpV and the pzpy-like ligands were measured *via* a fluorescence method. A stock solution of the pzpy-like ligand (1×10^{-2} mol L^{-1}) was prepared by ethanol, and diluted with HEPES buffer solution (0.1 mol L^{-1}, pH = 7.0) to 1×10^{-4} mol L^{-1} for testing, while bpV was diluted by HEPES buffer solution to 2.5×10^{-2} mol L^{-1}. A 2.5 mL pzpy-like ligand test solution was titrated by successive additions (10 μL) of bpV solution with concentrations varying from 0 to 12×10^{-4} mol L^{-1} at 30 °C.

Detailed spectroscopic measurement results may be found in ESI.†

Acknowledgements

This work was supported by the NSF of China (21172066, 21201062, and 51103122), the Ministry of Science and Technology (2011CB808505), Scientific Research Fund of Hunan Provincial Education Department (12K101), Hunan Provincial Natural Science Foundation of China (11JJ2007), the Opening Project of State Key Laboratory of Physical Chemistry of Solid Surfaces (Xiamen University, 201309), and Aid Program for Science and Technology Innovative Research Team in Higher Educational Institutions of Hunan Province.

References

1 (*a*) K. H. Thompson and C. Orvig, *Science*, 2003, **300**, 936–939; (*b*) K. H. Thompson and C. Orvig, *J. Inorg. Biochem.*, 2006, **100**, 1925–1935; (*c*) K. H. Thompson, J. H. McNeill and C. Orvig, *Chem. Rev.*, 1999, **99**, 2561–2572.

2 (*a*) D. C. Crans, J. J. Smee, E. Gaidamauskas and L. Yang, *Chem. Rev.*, 2004, **104**, 849–902; (*b*) D. C. Crans, A. D. Keramidas, S. S. Amin, O. P. Anderson and S. M. Miller, *J. Chem. Soc., Dalton Trans.*, 1997, 2799–2812.

3 D. C. Crans, A. D. Keramidas, H. Hoover-Litty, O. P. Anderson, M. M. Miller, L. M. Lemoine, S. Pleasic-Williams, M. Vandenberg, A. J. Rossomando and L. J. Sweet, *J. Am. Chem. Soc.*, 1997, **119**, 5447–5448.

4 A. Butler and J. V. Walker, *Chem. Rev.*, 1993, **93**, 1937–1944.

5 B. I. Posner, R. Faure, J. W. Burgess, A. P. Bevan, D. Lachance, G. Y. Zhang-Sund, I. G. Fantus, J. B. Ng, D. A. Hall, B. S. Lum and A. Shaver, *J. Biol. Chem.*, 1994, **269**, 4596–4604.

6 (*a*) J. H. Hwang, R. K. Larson and M. M. Abu-Omar, *Inorg. Chem.*, 2003, **42**, 7967–7977; (*b*) M. Sam, J. H. Hwang, G. Chanfreau and M. M. Abu-Omar, *Inorg. Chem.*, 2004, **43**, 8447–8455; (*c*) D. W. J. Kwong, O. Y. Chan, R. N. S. Wong, S. M. Musser, L. Vaca and S. I. Chan, *Inorg. Chem.*, 1997, **36**, 1276–1277.

7 (*a*) H. Sugiyama, S. Matsugo, T. Konishi, T. Takamura, S. Kaneko, Y. Kubo, K. Sato and K. Kanamori, *Chem. Lett.*, 2012, **41**, 377–379; (*b*) L. Z. Geng, J. Xing and Y. Z. Zhou, *Chin. J. Struct. Chem.*, 2012, **31**, 185–190; (*c*) M. Kaliva, C. Gabriel, C. P. Raptopoulou, A. Terzis, G. Voyiatzis, M. Zervou, C. Mateescu and A. Salifoglou, *Inorg. Chem.*, 2011, **50**, 11423–11436; (*d*) C. R. Waidmann, A. G. DiPasquale and J. M. Mayer, *Inorg. Chem.*, 2010, **49**, 2383–2391.

8 (*a*) V. Conte, F. Di Furia and S. Moro, *Tetrahedron Lett.*, 1994, **35**, 7429–7432; (*b*) M. Andersson, V. Conte, F. Di Furia and S. Moro, *Tetrahedron Lett.*, 1995, **36**, 2675–2678; (*c*) V. Conte, F. Di Furia, S. Moro and S. Rabbolini, *J. Mol. Catal.*, 1996, **113**, 175–184; (*d*) V. Conte and B. Floris, *Inorg. Chim. Acta*, 2010, **363**, 1935–1946; (*e*) V. Conte, F. Fabbianesi, B. Floris, P. Galloni, D. Sordi, I. W. C. E. Arends, M. Bonchio, D. Rehder and D. Bogdal, *Pure Appl. Chem.*, 2009, **81**, 1265–1277.

9 (*a*) G. J. Colpas, B. J. Hamstra, J. W. Kampf and V. L. Pecoraro, *J. Am. Chem. Soc.*, 1994, **116**, 3627–3628; (*b*) G. J. Colpas, B. J. Hamstra, J. W. Kampf and V. L. Pecoraro, *J. Am. Chem. Soc.*, 1996, **118**, 3469–3478; (*c*) T. S. Smith and V. L. Pecoraro, *Inorg. Chem.*, 2002, **41**, 6754–6760; (*d*) G. Zampella, P. Fantucci, V. L. Pecoraro and L. De Gioia, *Inorg. Chem.*, 2006, **45**, 7133–7143.

10 A. Shaver, J. B. Ng, D. A. Hall, B. S. Lum and B. I. Posner, *Inorg. Chem.*, 1993, **32**, 3109–3113.

11 (*a*) X. Y. Yu, X. Xu and Z. Chen, *Int. J. Mass Spectrom.*, 2008, **269**, 138–144; (*b*) X. Y. Yu, S. H. Cai, X. Xu and Z. Chen, *Inorg. Chem.*, 2005, **44**, 6755–6762; (*c*) X. Y. Yu, S. H. Cai and Z. Chen, *J. Inorg. Biochem.*, 2005, **99**, 1945–1951; (*d*) X. Y. Yu, J. Zhang, S. H. Cai, P. G. Yi and Z. Chen, *Spectrochim. Acta, Part A*, 2009, **72**, 965–969; (*e*) B. R. Zeng, R. Q. Fu, S. H. Cai, J. Zhang and Z. Chen, *Inorg. Chim. Acta*, 2011, **365**, 119–126; (*f*) B. R. Zeng, R. Q. Fu, S. H. Cai and Z. Chen, *Inorg. Chem. Commun.*, 2009, **12**, 1259–1262.

12 (*a*) A. Gorzsas, I. Anderson and L. Pettersson, *J. Inorg. Biochem.*, 2009, **103**, 517–526; (*b*) L. Pettersson, I. Andersson and A. Gorzsas, *Coord. Chem. Rev.*, 2003, **237**, 77–87; (*c*) I. Andersson, A. Gorzsas and L. Pettersson, *Dalton*

Trans., 2004, 421–428; (*d*) H. Schmidt, I. Andersson, D. Rehder and L. Pettersson, *J. Inorg. Biochem.*, 2000, **80**, 149–151; (*e*) H. Schmidt, I. Andersson, D. Rehder and L. Pettersson, *Chem.–Eur. J.*, 2001, **7**, 251–257; (*f*) A. Gorzsas, I. Andersson and L. Pettersson, *Dalton Trans.*, 2003, 2503–2511; (*g*) M. Časný and D. Rehder, *Dalton Trans.*, 2004, 839–846; (*h*) X. Y. Yu, P. G. Yi, D. H. Ji, B. R. Zeng, X. F. Li and X. Xu, *Dalton Trans.*, 2012, **41**, 3684–3694.

13 (*a*) A. M. Kutasi, D. R. Turner, B. Moubaraki, S. R. Batten and K. S. Murray, *Dalton Trans.*, 2011, **40**, 12358–12367; (*b*) S. R. Batten, J. Bjernemose, P. Jensen, B. A. Leita, K. S. Murray, B. Moubaraki, J. P. Smith and H. Toftlund, *Dalton Trans.*, 2004, 3370–3375; (*c*) X. T. Zhang, X. Y. Wu, D. F. Sun, P. H. Wei, Z. H. Ni, J. M. Dou, D. C. Li, C. W. Shi and B. Hu, *Sci. China Chem.*, 2010, **53**, 2285–2290; (*d*) V. Mishra, F. Lloret and R. Mukherjee, *Eur. J. Inorg. Chem.*, 2007, 2161–2170; (*e*) J. S. Uber, Y. Vogels, D. van den Helder, I. Mutikainen, U. Turpeinen, W. T. Fu, O. Roubeau, P. Gamez and J. Reedijk, *Eur. J. Inorg. Chem.*, 2007, 4197–4206; (*f*) T. L. Hu, R. Q. Zou, J. R. Li and X. H. Bu, *Dalton Trans.*, 2008, 1302–1311; (*g*) A. C. Coelho, M. Nolasco, S. S. Balula, M. M. Antunes, C. C. L. Pereira, F. A. A. Paz, A. A. Valente, M. Pillinger, P. Ribeiro-Claro, J. Klinowski and I. S. Goncalves, *Inorg. Chem.*, 2011, **50**, 525–538; (*h*) A. P. Martinez, M. J. Fabra, M. P. Garcia, F. J. Lahoz, L. A. Oro and S. J. Teat, *Inorg. Chim. Acta*, 2005, **358**, 1635–1644; (*i*) T. Jozak, D. Zabel, A. Schubert, Y. Sun and W. R. Thiel, *Eur. J. Inorg. Chem.*, 2010, 5135–5145; (*j*) L. Holland, W. Z. Shen, P. von Grebe, P. J. S. Miguel, F. Pichierri, A. Springer, C. A. Schalley and B. Lippert, *Dalton Trans.*, 2011, **40**, 5159–5161; (*k*) K. Suntharalingam, D. Gupta, P. J. S. Miguel, B. Lippert and R. Vilar, *Chem.–Eur. J.*, 2010, **16**, 3613–3616.

14 (*a*) A. Shaver, D. A. Hall, J. B. Ng, A. M. Lebuis, R. C. Hynes and B. I. Posner, *Inorg. Chim. Acta*, 1995, **229**, 253–260; (*b*) P. Schwendt, M. Ahmed and J. Marek, *Inorg. Chem. Commun.*, 2004, **7**, 631–633; (*c*) J. Tatiersky, P. Schwendt, J. Marek and M. Sivak, *New J. Chem.*, 2004, **28**, 127–133; (*d*) D. Begin, F. W. B. Einstein and J. Field, *Inorg. Chem.*, 1975, **14**, 1785–1790; (*e*) S. Helga and S. Rolf, *Acta Chem. Scand.*, 1983, **A37**, 553–559.

15 (*a*) X. Y. Yu, R. H. Liu, H. L. Peng, H. W. Huang, X. F. Li, B. S. Zheng, P. G. Yi and Z. Chen, *Spectrochim. Acta, Part A*, 2010, **75**, 1095–1099; (*b*) X. Y. Yu, F. X. Yang, D. H. Ji, J. M. Zhou, R. H. Liu;, G. B. Li, X. F. Li, J. Chen, H. W. Huang and P. G. Yi, *Spectrochim. Acta, Part A*, 2010, **77**, 816–820; (*c*) X. Y. Yu, D. H. Ji, R. H. Liu, F. X. Yang, J. Xie, J. M. Zhou, X. F. Li and P. G. Yi, *J. Coord. Chem.*, 2010, **63**, 1555–1562; (*d*) R. J. Zeng, Z. X. Wang, X. F. Li, J. Xie and X. Y. Yu, *J. Coord. Chem.*, 2010, **63**, 498–504.

16 D. Rehder, T. Polenova and M. Bühl, *Annu. Rep. NMR Spectrosc.*, 2007, **62**, 50–114.

17 (*a*) H. A. Benesi and J. H. Hildebrand, *J. Am. Chem. Soc.*, 1949, **71**, 2703–2707; (*b*) C. Yang, L. Liu, T. W. Mu and Q. X. Guo, *Anal. Sci.*, 2000, **16**, 537–539; (*c*) R. Rajamohan, S. Kothai Nayaki and M. Swaminathan, *J. Solution Chem.*, 2011, **40**, 803–817.

18 V. Conte, O. Bortolini, M. Carraro and S. Moro, *J. Inorg. Biochem.*, 2000, **80**, 41–49.

19 (*a*) F. Wang and A. W. Schwabacher, *Tetrahedron Lett.*, 1999, **40**, 4779–4782; (*b*) J. S. Uber, Y. Vogels, D. van den Helder, I. Mutikainen, U. Turpeinen, W. T. Fu, O. Roubeau, P. Gamez and J. Reedijk, *Eur. J. Inorg. Chem.*, 2007, **26**, 4197–4206; (*c*) W. R. Thiel, M. Angstl and T. Priermeier, *Chem. Ber.*, 1994, **127**, 2373–2379; (*d*) H. Zhang, Q. Cai and D. W. Ma, *J. Org. Chem.*, 2005, **70**, 5164–5173.